Unclassified
SECURITY CLASSIFICATION OF THIS PAGE

AD-A222 371

REPORT DOCUMENTATION PAGE

1a. REPORT SECURITY CLASSIFICATION Unclassified	1b RESTRICTIVE MARKINGS None
SECURITY CLASSIFICATION AUTHORITY	3 DISTRIBUTION / AVAILABILITY OF REPORT Approved for public release and sale. Distribution unlimited.
DECLASSIFICATION / DOWNGRADING SCHEDULE	
PERFORMING ORGANIZATION REPORT NUMBER(S) ONR Technical Report No. 18	5 MONITORING ORGANIZATION REPORT NUMBER(S)
NAME OF PERFORMING ORGANIZATION University of Utah 6b OFFICE SYMBOL (If applicable)	7a NAME OF MONITORING ORGANIZATION
ADDRESS (City, State, and ZIP Code) Department of Chemistry Henry Eyring Building Salt Lake City, UT 84112	7b ADDRESS (City, State, and ZIP Code)
NAME OF FUNDING / SPONSORING ORGANIZATION Office of Naval Research 8b OFFICE SYMBOL (If applicable)	9 PROCUREMENT INSTRUMENT IDENTIFICATION NUMBER N00014-89-J-1412
8c. ADDRESS (City, State, and ZIP Code) Chemistry Program, Code 1113 800 N. Quincy Street Arlington, VA 22217	10 SOURCE OF FUNDING NUMBERS PROGRAM ELEMENT NO / PROJECT NO. / TASK NO / WORK UNIT ACCESSION NO

11 TITLE (Include Security Classification)
Measurements of Energy Dispersion at Liquid-Solid Interfaces: Fluorescence Quenching of Pyrene Bound to Fumed Silica

12 PERSONAL AUTHOR(S)
A. L. Wong, J. M. Harris, D. B. Marshall

13a. TYPE OF REPORT	13b TIME COVERED	14 DATE OF REPORT (Year, Month, Day)	15 PAGE COUNT
Technical	FROM 6/89 TO 5/90	May 29, 1990	32

16. SUPPLEMENTARY NOTATION

17 COSATI CODES			18 SUBJECT TERMS (Continue on reverse if necessary and identify by block number)
FIELD	GROUP	SUB-GROUP	Surface energetics; reaction kinetics at liquid/solid interfaces.

19. ABSTRACT (Continue on reverse if necessary and identify by block number)

Attached.

20 DISTRIBUTION / AVAILABILITY OF ABSTRACT	21 ABSTRACT SECURITY CLASSIFICATION
☒ UNCLASSIFIED/UNLIMITED ☐ SAME AS RPT ☐ DTIC USERS	Unclassified
22a NAME OF RESPONSIBLE INDIVIDUAL Joel M. Harris	22b TELEPHONE (Include Area Code) (801)581-3585 / 22c OFFICE SYMBOL

DD FORM 1473, 84 MAR — 83 APR edition may be used until exhausted. All other editions are obsolete

SECURITY CLASSIFICATION OF THIS PAGE
Unclassified

OFFICE OF NAVAL RESEARCH

Grant No: N00014-89-J-1412

R&T Code 413a005---03

Technical Report No. 18

Measurements of Energy Dispersion at Liquid-Solid Interfaces: Fluorescence Quenching of Pyrene Bound to Fumed Silica

Prepared for publication in Canadian Journal of Physics

by

A. L. Wong, J. M. Harris and D. B. Marshall

Department of Chemistry
University of Utah
Salt Lake City, UT 84112

and

Department of Chemistry and Biochemistry
Utah State University
Logan, UT 84322

May 29, 1990

MEASUREMENTS OF ENERGY DISPERSION AT LIQUID-SOLID INTERFACES: FLUORESCENCE QUENCHING OF PYRENE BOUND TO FUMED SILICA

A. L. Wong and J. M. Harris*
Department of Chemistry
University of Utah
Salt Lake City, UT 84112 USA

D. B. Marshall*
Department of Chemistry and Biochemistry
Utah State University
Logan, UT 84322-0300 USA

Abstract

The observation of a stretched exponential response in chemical kinetics at solid-liquid interfaces is an indicator of solid surface disorder. In this contribution, we review earlier relaxation kinetics studies of solid surface disorder and the statistical criteria analyzing kinetic data which are not single exponential. We draw on these concepts to interpret the fluorescence decay kinetics of pyrene covalently attached to the surface of fumed silica particles which are suspended in methanol. This surface probe exhibits stretched exponential behavior of the form $f(t) = \exp[-(kt)^{\beta}]$ in the decay of its excited-state populations. The addition of iodine quencher increases the average decay rate but does not alter the nonlinear exponent, β. These results, along with the diffusional length of the iodine quencher, the photophysics of the probe, and the chemistry of the interface, indicate that the kinetic inhomogeneity is dominated by dispersion of surface energies, rather than by diffusional excursions of the quencher on a fractally aggregated surface. Numerical Laplace inversion of the experimental decay curves is used to determine the distribution of rates which reveal that the quenching process is inhomogeneous and correlated with the unquenched decay rates of the probe.

Index Classification: 82.40

Introduction

Chemically modified silicas are important materials in a variety of applications, including reactions with immobilized reagents or catalysts and chemical separations. Silica has been described as both geometrically and energetically heterogeneous. Geometric characteristics are related to surface topography and morphology while surface energetic properties are related to the nature and distribution of silanols on the silica surface. Questions about the geometrical and energetic characteristics of chemically modified surfaces with respect to binding and adsorption of molecules has motivated the development of tools for investigating these characteristics. Relaxation kinetic measurements of adsorption-desorption reactions and fluorescence decay kinetics of surface-bound probe molecules can provide information about the geometric and energetic characteristics of disordered surfaces that is difficult to obtain by other means. Kinetic curves obtained from relaxation measurements on homogeneous systems are single exponential regardless of the underlying reaction mechanism, if the perturbation size is kept sufficiently small. This "linearization of the rate equation" is possible due to terms of square or higher powers in the perturbation being negligibly small (1). For energetically disordered surfaces, there will be a distribution of surface interactions, which will be reflected in the relaxation kinetics as a distribution of reaction rates. Time-resolved fluorescence emission from surface-bound probes on disordered surfaces can also be modeled as a distribution of first-order decay rates. A sum of first-order rate processes yields an experimental decay curve which is the Laplace transform of the rate distribution. Thus, Laplace inversion of the decay curve yields the rate distribution, which can be related to the underlying surface disorder (2).

An alternative interpretation of data from relaxation and fluorescence quenching kinetic experiments on heterogeneous surfaces is to treat the data as being of "stretched exponential" form, $f(t) = \exp[-(kt)^{\beta}]$, and fit the data to the appropriate stretched exponential function. The problem then becomes one of assigning physical meaning to the values of the parameters obtained. Stretched exponential behavior has been observed in a wide variety of experiments, with more recent examples noted in direct energy transfer on silicas (3) and in free radical abstraction reactions in glasses (4). Kinetics in fractal environments will also exhibit time-dependent rate "constants", resulting in stretched exponential decays. For example, second-order dimerization reactions in membranes exhibit rate laws of the form $R = kt^{-h}c^2$, with $h = 1-d_s/2$ (5), where d_s is the fracton or "spectral" dimension (6).

The choice between fitting multiexponential data to a stretched exponential or treating the data as the Laplace transform of an underlying distribution would depend on the physical model that is appropriate for the system. Unfortunately, in many experimental cases the appropriate model is initially poorly defined or unknown. Many experiments reported to date fail to address the question of whether observed heterogeneity arises from geometric factors, energetic disorder, or both. Even the choice between an ordered (discrete distribution) and a disordered (continuous) distribution can be problematic.

When first-order kinetics occur in multicomponent or dispersive systems and when the resolving power of the experiment is less than the time- or energy-based separation between components of the system, the data represent an essentially continuous sum of the single exponential elements to yield a continuous exponential process. As noted above, since a single exponential is the kernel of the Laplace transform, the analysis of the data for the contin-

uous exponential case becomes a problem in inversion of the Laplace transform. Laplace inversion can be done analytically, by fitting the decay curve to some analytical function and solving for its Laplace transform pair, or numerically, without a prior choice of the mathematical form of the decay. Exponential-like curves are members of the class of "extreme value distributions" and thus exhibit instability in either analytical solutions or in numerical inversion.

Numerical inversion seems preferable in circumstances where an a priori choice of a model cannot be made, since more control can be exercised during the inversion process by applying reasonable, physical constraints to the solution. By applying the technique of constrained regularization, the solution is limited to values of the rate constants that are non-negative and non-zero only over an experimentally reasonable range. With the additional application of the principle of parsimony, wherein the least detailed solution consistent with the data is chosen, direct numerical inversion can provide stable, physically reasonable results at the cost of larger variance in the resulting distribution and possible "blurring" of real detail in the distribution (7).

Results of a series of numerical tests where fits of synthetic data to discrete versus continuous models were compared on statistical grounds have shown that the ability to distinguish between these models is strongly dependent on the noise level in the data (8). Data should be collected with average noise levels less than 0.5%, or a signal-to-noise ratio greater than 400, if the discrimination between single exponential and continuous exponential models is required. If, in the worst case, a discrete, multiexponential model with closely spaced components is a significant possibility, then data should be collected with noise levels of 0.1% or lower, corresponding to a signal-to-noise ratio of 2,000 or higher (8). These requirements place severe

constraints on the interpretation of data from complicated systems, and thus represent a practical problem in efforts to extract geometric and energetic disorder of surfaces from relaxation kinetics, fluorescence quenching, or similar experiments.

Another major difficulty in properly analyzing experimental data from kinetic measurements in disordered media is that many different fundamental effects are expected to give rise to identical observations. Spatial distributions of reaction sites, fractal geometries, or distributions of desorption ("waiting") times all are expected to result in stretched exponential behavior (9). When both temporal (energetic) and structural factors that lead to stretched exponential behavior are present, the exponent of the decay contains multiplicative exponents for both temporal and structural effects (10) which are impossible to disentangle in most cases. An exception is predicted from continuous-time random walk studies (10) of the motion of reactive walkers on fractal lattices (structural effect), where the walkers also have a distribution of waiting times (energetic effect). These studies have shown that it is possible to distinguish the two effects for "trapping" minority species A which moves freely over a surface having fixed quenching sites B. The dependence of the decay kinetics of A on the density of traps B indicates that it should be possible to distinguish the dispersion in adsorption energy from the time dependence and the spectral dimension from the trap concentration dependence (10).

Given the theoretical and statistical difficulties involved in treating data from disordered systems, it is imperative that experimental probes remove as much of the ambiguity as possible. A previous relaxation kinetics experiment involved an octadecylated microporous silica suspended in methanol (11).

The anion of the ion pair was a fluorescent indicator that only exhibited measurable fluorescence when entrained in the octadecyl groups. Measurement of the desorption rate showed a dispersion in the rate constant that, because of the indicator characteristics, was most likely due to a chemical heterogeneity in the free energy of ion pair-octadecyl group binding rather than factors related to diffusional motion of the ion pair in solution or along the surface. From the calculated dispersion in desorption rate constant, a dispersion in the free energy of interaction was determined by Laplace inversion (11).

In contrast, relaxation measurements of the sorption-desorption kinetics of anthranilic acid with suspensions of octadecyl microporous silica are more analogous to the trapping problem considered above. Here, the free solution anionic form of the indicator is detected, and the adsorption-desorption of the neutral, protonated form is detected indirectly via coupling with the acid association-dissociation reaction. The relaxation rate of the signal is now sensitive to diffusional motion of the adsorbing species up to and along the surface. The early part of the relaxation decay curves is of stretched exponential form. Some evidence is seen for a crossover to algebraic decay in the tails of the relaxation decay curves (J. W. Burns and D. B. Marshall, work in progress).

Fluorescence probe methods for chemically modified silica surfaces have been developed which provide another means of probing energetic and geometric disorder. Here, pyrene is covalently attached to the surface and the spectral (12) and temporal (13) characteristics of its fluorescence are measured. Quenching of anchored pyrene, when the diffusional length of the quencher is long relative to the scale of interesting morphological features of the interface, could provide useful information about geometric disorder. The

present study describes fluorescence decay rate studies of pyrene covalently attached through a propylsilyl linkage to spherical fumed silica particles in methanol suspensions. Laplace inversion is used to recover the underlying fluorescence decay rate distributions in the presence and absence of a quencher (iodine) in solution. Analysis of the decay curves provide rate distributions which are distinguishable from a homogeneous bimolecular quenching process. Two mechanisms for the inhomogeneous fluorescence quenching of an immobilized probe on silica are proposed which would account for the observations.

Experimental

Materials: The synthesis of 3-(1-pyrenyl)-propyldimethyl-monochlorosilane (3PPS) and its subsequent reaction with the silica are described in detail elsewhere (14). "Fumed" or "pyrogenic" silicon dioxide was purchased from Cab-O-Sil, type LS-90. This material is produced by hydrolysis of silicon tetrachloride vapor in a hydrogen and oxygen flame. The fumed silica (mean particle diameter 0.024 μm and nitrogen BET surface area of 90 m^2/g) was used in the preparation of the pyrene-labeled material. Spectral grade chloroform dried and stored over molecular sieves was used in the derivatization of the silica. Spectral grade solvents, chloroform, tetrahydrofuran, acetonitrile, methanol, and acetone, were used to wash the chemically modified silica. Methanol (EM Science, Omnisolv) and iodine (Mallinchrodt, resublimed crystals 99.91%) were used without further purification. Solutions of varying iodine concentrations between 0.2 mM and 0.8 mM in methanol were prepared using standard volumetric techniques.

Surface Analysis: Fluorescence emission spectra of immobilized pyrene on fumed silica particles were recorded and used to infer local proximity of bound fluorophores on the surface. Spectra were collected with a Farrand Optical

Scanning Spectrophotometer (model 801) at an excitation wavelength of 305 nm while the emission monochromator was scanned from 350 to 500 nm.

Chromatographic retention measurements of iodine on silica surfaces in methanol were obtained utilizing a column packed with porous silica (Analytichem International, 25cm x 2.51mm). A flow rate of 1 mL/min was controlled by a Beckman Model 110A chromatographic pump and optical absorption at a single wavelength (254 nm) was measured to detect the eluent using a Beckman Model 153. Retention values of iodine on the silica column are reported relative to pentane, which has a negligible affinity for the silica surface (22).

Fluorescence Decays: Fluorescence decay curves were obtained from slurries of 1% pyrene-labeled silica in methanol by weight. Samples were prepared by sonicating the silica for 30 minutes in solvent. Oxygen was removed from the sample by three freeze-pump-thaw cycles, after which the slurry was allowed to equilibrate at room temperature for 2 hours prior to collection of fluorescence transients. I_2 concentrations over a range of 10^{-4} M to 10^{-3} M in methanol were used in the study. The decay curves were obtained by single-photon-counting employing the laser fluorimeter described in reference 15. Each fluorescence transient was analyzed by a nonlinear least-squares algorithm which employed a Marquardt search (16) to minimize the Chi-square ($\chi 2$) statistics. The reported decay parameters were averaged from 8 different transients at each quencher concentration.

Decay curves were fitted to a stretched exponential model both by assigning the stretched exponential parameter ß equal to 2/3 and by allowing ß to float as an adjustable parameter:

$$I = I_0 \exp[-(t/\tau)\beta] \qquad [1]$$

where I_o is the intensity at t = 0, and τ is the decay time. An F-test (17) was used to determine whether significant improvement in the variance of the fit resulted from floating the parameter B, and is given by:

$$F = [\chi^2(n-1) - \chi^2(n)] * [N-n-1]/\chi^2(n) \qquad [2]$$

In equation 2, N equals the number of data points and, n = 3 is the number of parameters including B. The ratios of the variances F were subsequently compared to the critical values at the 95% confidence level for $\nu 1 = 1$ and $\nu 2 = N-n-1$ degrees of freedom. Only the last 85% of the decay curves (85 - 480 ns) were included in the time-domain analysis due to silica background fluorescence, which decreases rapidly to less than 1% of the pyrene signal within the first 80 ns. The fluorescence decay curves were also analyzed as a distribution of first-order decay rates using the numerical Laplace inversion program CONTIN (18). Here, the entire decay curves was analyzed since silica background fluorescence is resolved from the pyrene signal on the basis of its faster decay rate. The distributions were truncated at $k = 2.8 \times 10^7$ sec^{-1} to avoid interpreting this background and a numerical artifact which arises from using a disrete number of data points to represent a continuous decay process.

Results and Discussion

The fluorescence of pyrene covalently bound on the spherical surface of fumed silica suspended in a methanol solution containing iodine does not follow a single-exponential decay, as shown in Figures 1(a) and 1(b). Attempts to fit the fluorescence decay data to a sum of two and three exponentials were equally unsuccessful. Concern could be raised as to whether this behavior could be attributed to formation of excited-state dimers (excimers), since excimer emission from silica-bound 3PPS has been demonstrated (12,13). This is not the case in the present data as evidenced by the absence of excimer emission at ~470 nm (less than 1% compared to monomer emission). The amount of 3PPS reagent bound to the silica surface was less than 0.4 μmoles/m^2. Based on studies of the excimer formation under similar conditions (12), this surface coverage should produce excimer/monomer emission ratios of less than 2%.

Fitting the decay data to a stretched exponential function (Equation 1), with the exponent β fixed at 0.67 resulted in considerable improvement (χ^2 < 1.3), as shown in Figures 1(a) and 1(c). Including β as a variable in the nonlinear least-squares algorithm allows the value of the parameter to be optimized. This approach proved unreliable for analysis of individual decay curves since the optimum values of β and the lifetime τ are highly correlated. Nevertheless, an average obtained from the analysis of 32 decay curves, of the type shown in Figure 1, indicates that β = 0.67 ± 0.1.

Bimolecular processes which occur in a fractal environment exhibit stretched exponential behavior. The spherical 24 nm silica particles used in this study are known to form fractal aggregates in solution (19,20). The theoretical predictions for the value of β for the case of a random walker moving up to or along such an aggregate is 2/3 (d_s = 4/3, β = d_s/2 = 2/3)

(6,10). It is thus tempting to attribute the observation of $\beta = 0.67$ to geometric factors of the silica aggregate influencing the transport of the quencher to the excited-state.

Fluorescence decays of immobilized pyrene on silica suspended in methanol without quencher also exhibited stretched exponential behavior, as shown in Figure 2. Surprisingly, the optimum value of β remains constant at 0.67. One might expect that the exponent β in this case would equal one since collisional deactivation of the excited-state by quencher is absent so that the decay should not be sensitive to transport phenomena. The constancy of β, even in the absence of a quencher, raises questions about the role of fractal transport even when the decay kinetics are dominated by quenching. Chromatographic measurements of the partitioning of iodine between bare silica and methanol show only weak adsorption of iodine on the silica from methanol solution; the fraction of iodine adsorbed to the surface of the suspended silica is estimated (30) to be $< 5 \times 10^{-3}$ % from these results. Neglecting for the moment any role which this weak adsorption play in the transport of the quencher, the diffusional length of the quencher in solution can be estimated using Einstein's relation $\bar{x} = (2Dt)^{1/2}$ and the diffusion coefficient of iodine D in free solution, measured experimentally (23). Over the time scale of the experiment (given by the unquenched fluorescence lifetime of surface bound pyrene), the diffusional length of I_2 in free solution is 28 nm, only slightly larger than the diameter of the primary spherical silica particles. Quenching of anchored probes, when the diffusion length is long relative to the length scale of morphological features of the interface, should provide useful information about the geometry of those features. Given that the diffusional length of iodine is too small in this case to sample the fractal aggregate of

silica particles it is more reasonable to attribute the stretched exponential behavior to an environmental heterogeneity of pyrene on the surface which causes a dispersion in the excited-state lifetime. This conclusion is reinforced by the observation that the stretched exponential decay of the pyrene probe in the absence of quencher exhibited the same 2/3 dependence in its exponent.

The temporal characteristics of fluorescence from adsorbed pyrene are sensitive to local surface energy disorder of silica (21). Surface inhomogeneities on silica have also been observed to influence the covalent bonding of molecules to the surface (13). The dispersion in surface energies is most likely related to the local density of surface hydroxyls or silanols on the silica surface. A naive representation of evenly distributed silanols on silica is being replaced by a picture where high densities of hydroxyl exist in "clusters" giving rise to regions of higher reactivity (13). Adsorptive interactions between pyrene and surface silanols alter the electron density and symmetry of a surface-bound pyrene probe (24). Such perturbations can promote mixing in pyrene between the lowest energy short axis-polarized B_{2u} excited state and the long axis-polarized B_{1u} state at slightly higher energy (25). Radiative transitions from this latter state are more strongly allowed; thus the excited state lifetime of pyrene depends on the degree of state mixing which is sensitive to local environment. A dispersion of surface energies (unequal density of silanols), which interact with the excited states of pyrene through adsorption, results in a dispersion of radiative rates.

If the dispersion of fluorescence lifetimes is indeed due to a distribution in the interactions of pyrene with the silica surface, it is appropriate to treat the data as a weighted sum of first-order decay curves. A method of

recovering the underlying rate constant distribution is through Laplace inversion of the decay data. The rate constant distribution for the entire data transient of Figure 2 is shown in Figure 3(i). The distribution is noticeably asymmetric, with a tail of larger rate constants (shorter lifetimes). The mean of the pyrene decay rate distribution is $\langle k_o \rangle = 5.53 \times 10^6\ s^{-1}$ (corresponding to a lifetime of 181 ns). The rate constants from Figure 3(i) are physically reasonable for the surface-bound propylpyrene molecule in different environments. The fluorescence lifetime of 1-methylpyrene (a free solution analog to the surface bound probe) depends on solvent polarity. Using the same techniques to determine the fluorescence decay rate of this compound in free solution, we find that it decays as a single exponential with lifetimes which vary from 102 ns ($k_o = 9.80 \times 10^6\ s^{-1}$) in water to 220 ns ($k_o = 4.54 \times 10^6\ s^{-1}$) in hexane.

The effects of a dispersion in surface energies on rates of fluorescence quenching are more challenging to describe. To assess the rate of quenching, fluorescence transients from immobilized pyrene on silica were collected over a range of iodine concentrations and fit to Equation 1, with β fixed at 0.67. The decay rates increased linearly with concentration, as predicted by a collisional quenching model described by the Stern-Volmer equation:

$$1/\tau = k_o + k_q[Q] \qquad [3]$$

where k_o is the radiative decay rate of pyrene in the absence of quencher, k_q the bimolecular quenching rate constant, and [Q] is the concentration of iodine. A plot of the inverse lifetime ($1/\tau$) versus iodine concentration is shown in Figure 4 (squares). The bimolecular rate constant, given by the slope of the best fit straight line (linear correlation coefficient, $r = 0.9999$), is $k_q = 1.87(\pm 0.02) \times 10^{10}\ M^{-1}\ s^{-1}$. This quenching rate is indistinguishable from

the quenching rate of 1-methylpyrene by iodine in free solution (23), which is a surprising result since no correction for the surface-immobilization of the fluorophore was included in the determination of k_q. Surface immobilization affects the relative motion and accessibility of reactants. The expected reduction in rate at or near a surface is proportional to the volume excluded by the surface and the fraction of the diffusion carried by the excited-state (23,26,27). In the present case, the expected reduction in rate of quenching of the immobilized probe is approximately a factor of 0.5. The collisional process may be facilitated, however, through "indirect" reaction pathways (physisorbtion of quencher followed by rapid surface diffusion to pyrene) (28), whereby weak adsorption of iodine results in an enhanced rate.

Using a constant value of $\beta = 2/3$, the quality of fit of the fluorescence decay curves was excellent over the range of iodine concentrations. Given an underlying distribution of emission rates for the pyrene probe, one might anticipate that at high concentrations of iodine (where the collisional quenching process dominates the decay) the value of β would be altered. Assuming a homogeneous quenching process of the inhomogeneous population of excited-states, the fluorescence intensity is given by (21):

$$I(t) = I_o \exp[-(k_o t)^{\beta} - k_q[Q]t] \qquad [4]$$

where k_o is the radiative decay rate in the absence of quencher, where the decay curves should approach a single exponential ($\beta = 1$) at high concentrations of quencher. Nonlinear least-squares fit of the time-dependent data, however, showed no systematic increase in β indicating that the quenching process is probably not homogeneous.

The results of Laplace inversion of the quenched fluorescence decay curves, provide further insight into the mechanism of fluorescence quenching.

The underlying decay rate distributions of immobilized pyrene on fumed silica upon addition of molecular iodine were recovered and characterized through the numerical inversion algorithm, as shown in Figure 3. The addition of iodine resulted in an expected shift of the decay rate distribution towards faster rates with increasing quencher concentration. These results can be used to check the fast quenching rate obtained by a stretched exponential fit of the time-dependent data. The mean decay rates, estimated from the first moment of the rate distributions in Figure 3, are offset from the stretched exponential ($1/\tau$) results due to differences in how the two methods weight the distribution, as seen in Figure 4. Nevertheless, the variation in the mean decay rates of the distributions with quencher concentration, k_q = 2.1 ($\pm$0.5) x 10^{10} M^{-1} s^{-1}, is indistinguishable from the quenching rate determined from the stretched exponential analysis of the time-dependent data. The results validate the large the bimolecular rate of quenching, comparable to free solution.

Another important observation that can be drawn from the rate distributions in Figure 3 is that the relative shapes of the distributions are invariant with quencher concentration. The increase in width of the distributions is proportional to the increase in decay rate as shown in Figure 5. These results provide additional evidence that β remains constant over the concentration range studied, since this nonlinear exponent parameter in the stretched exponential fit is related to the relative width of the corresponding rate distribution. The constancy of the β parameter is a strong indication that the quenching process is indeed inhomogeneous in this case, in contrast to other kinetic studies of inhomogeneous fluorescent populations where a homogeneous quenching model fit the results (3).

As an further check on this conclusion, theoretical rate distributions were constructed based upon homogeneous quenching of the initially inhomogeneous distribution of fluorescence decay rates (obtained from experimental data). The unquenched decay distribution can be represented as:

$$I(t) = \sum_i a_i \exp[-k_{oi}t] \Delta k \qquad [5]$$

where the parameters a_i and k_{oi}, the relative population and the decay rates, obtained by numerical Laplace inversion of the unquenched pyrene decay curve. Homogeneous quenching of this distibution of fluors by iodine can then be modeled as:

$$I(t) = \sum_i a_i \exp[-(k_{oi} + k_q[Q])t] \Delta k \qquad [6]$$

where the all populations are quenched at a constant rate ($k_q[Q]$). The results of this homogeneous quenching model are shown in Figure 6(a). This model predicts that the absolute width of the rate distribution remains constant upon addition of quencher (as shown in Figure 5). Since the average decay rate increases by $k_q[Q]$ according to Equation 6, the relative width of the rate distribution (width divided by the average) is predicted to decrease with increasing [Q], which is consistent with an increase in the β parameter discussed above.

The predictions of the homogeneous quenching model stand in sharp contrast with the experimental results, where the width of the distribution was found to increase with quencher concentration and the relative width of the distribution remained constant, indicating that the quenching process is <u>not</u> homogeneous. The faster rate portion of the measured rate distribution is shifted more upon

quenching than the slower decaying population as shown in Figure 3. This result indicates that fluorescence quenching of the short-lived excited state populations is more efficient than quenching of the longer-lived populations. We conclude, therefore, that the quenching rate constant, k_q, has a similar distribution as the unquenched decay rate (k_o), which is again consistent with the constant value of the ß parameter discussed above. There may also exist a correlation between the initial decay rate k_{oi} of a particular population and the quenching rate k_{qi} of that population.

Theoretical rate distributions were constructed to test the validity of an inhomogeneous quenching process where k_q and k_o are correlated. These rate distributions are based upon of the initial distribution of fluorescence decay rates obtained from experimental data (a_i, k_{oi}) and an assumption that the quenching rate of the ith population, k_{qi}, is proportional to the initial decay rate, $k_{qi} = (c\ k_{oi})$, where c is a proportionality constant. The resulting time-dependent fluorescence intensity predicted by this model is given by:

$$I(t) = \sum_i a_i \exp[-(1 + c\ [Q])k_{oi}t]\ \Delta k \qquad [7]$$

The rate distributions of this inhomogeneous quenching model were obtained by optimizing the single parameter, c, while comparing the results to those from the experiment. The predicted rate distributions for inhomogeneous quenching are plotted in Figure 6(b) and are very similar to the experimental results in Figure 3. The faster rate portion of the model distribution shifts more with higher quencher concentration than does the slower decaying population, as previously observed in the experimental rate distributions. In addition, the change in width of the modeled rate distribution agrees closely with the results obtained experimentally as shown in Figure 5. Small differences between the model and the experiment at the fastest rates arise from a

numerical artifact due to the continuous fluorescence decay process being represented by a discrete number of data points. This artifact only affects the experimental rate distributions since the predicted distributions were not subjected to numerical Laplace inversion.

The inhomogeneous nature of the quenching process where k_o and k_q are correlated may be related to the large value for quenching rate determined by the Stern-Volmer results in Figure 4. The fast rate of inhomogeneous quenching could be due to an indirect quenching mechanism, wherein quencher weakly physisorbs to the surface followed by surface diffusion to the bound pyrene. This process could cause a dispersion in quenching rates similar to the dispersion in the unquenched decay rate since both would be affected by the dispersion in adsorption energies. Chromatographic measurements of the partitioning of iodine between bare silica and methanol solvent indicated very weak retention of iodine on the silica surface. While the fraction of total iodine adsorbed by the colloid is indeed very small ($< 5x10^{-3}$%), the fraction responsible for indirect quenching could be much larger. Due to the small number of particles in suspension, only 3% of the iodine in solution is within the diffusional length of the surface of any silica particle. Thus, the fraction of adsorbed iodine when compared to the solution phase iodine which can access the surface within the fluorescence lifetime of the probe could be as large as 0.2%.

A dispersion in surface energetics (resulting in a 0.67 power dependence in the fluorescence decay kinetics) may be proportional to the dispersion in transport efficiency of weakly physisorbed iodine and hence carries the same power dependence. Additionally, iodine and pyrene may be selectively adsorbed at higher energy sites, which would result in a correlation between shorter

lifetimes (due to energetic perturbations), and a higher probability of colliding with quencher. Recall that numerical inversion of the quenched fluorescence decay curves indicate a bimolecular process whereby the shorter-lived populations of excited pyrene were quenched with greater efficiency.

An alternative explanation for the correlation between decay rate and quenching rate of a particular population of probe molecules could arise from the charge transfer nature of I_2 quenching of pyrene (28). This electron exchange quenching mechanism results in unusually high quenching rates in free solution. If iodine, an electron acceptor, interacts with electronically excited pyrene through a charge transfer mechanism, it is possible then to rationalize the correlation between a particular excited-state population of bound probe and quenching rate of that population. The perturbation of the excited-state symmetry which promotes faster radiative decay also affects the electron density or ionization potential of the excited state. The efficiency of quenching which proceeds through a charge transfer step would also be affected by changes in electron density on the pyrene ring. In this way, pyrene immobilized in a region of high silanol density would decay with a faster radiative rate and be quenched with greater efficiency through a charge transfer mechanism, producing a correlation between the short lived excited-state population of fluorophores and the quenching efficiency of that population. Further studies to distinguish between these two models are currently in progress.

Summary. The observation of a stretched exponential decay of fluorescence from immobilized pyrene on fumed silica can be attributed to surface disorder. The decay curves from fluorescence quenched by iodine in solution could be fit to a stretched exponential function having a nonlinear exponent, $\beta = 0.67$.

From these results alone, it would be tempting to ascribe the underlying disorder as geometric in origin which is influencing the transport of the quencher to the excited state. Eliminating the iodine quencher from solution did not, however, affect the stretched exponential form of the fluorescence decay curves from the surface-bound pyrene, and the parameter β remained 0.67. These observation, along with estimates of the diffusional length of the iodine quencher, knowledge of the photophysics of the fluorescent probe, and its sensitivity to the chemistry of the interface, appeared indicate that the kinetic inhomogeneity is dominated by dispersion of surface energies, and not by diffusional excursions of the quencher on a fractally aggregated surface.

To obtain an estimate of the rate distributions which arise from the dispersion in surface energies, the experimental decay curves were subjected to numerical Laplace inversion. These results confirmed observations from the stretched exponential analysis that the quenching process is inhomogeneous having a similar rate distribution as the unquenched decay of the probe. The results further indicated a correlation between the quenching rate and unquenched decay rate for given populations of probe molecules on the surface. This correlation appears to relate to the process by which iodine quenches surface-bound pyrene, a process which likely proceeds through a charge transfer interaction and may include an "indirect" or surface diffusion component.

Acknowledgements

This work was supported by the Office of Naval Research (JMH) and by the National Science Foundation (grant CHE-8719266, DBM). The authors express their appreciation to Isiah Warner for his help in locating a literature reference.

References

1. C. F. Bernasconi, Relaxation Kinetics. Academic Press, New York, NY. 1976.
2. W. Siebrand and T. A. Wildman. Acc. Chem. Res. 19, 238 (1986).
3. P. Levitz, J. M. Drake, and J. Klafter. In Molecular Dynamics in Restricted Geometries. Edited by J. Klafter and J. M. Drake. John Wiley & Sons, New York, NY. 1989. pp. 165-195.
4. T. Doba, K. U. Ingold, W. Siebrand and T. A. Wildman, Farad. Discuss. Chem. Soc., 78, 175 (1984).
5. J. Prasad and R. Kopelman. J. Phys. Chem. 91, 265 (1987).
6. S. Alexander and R. Orbach, J. Phys. (Paris) Lett., 43, L625 (1982).
7. S. W. Provencher. Comput. Phys. Commun. 27, 213 (1982).
8. D. B. Marshall. Anal. Chem. 61, 660 (1989).
9. J. Klafter and M. F. Shlesinger. Proc. Natl. Acad. Sci. USA 83, 848 (1986).
10. A. Blumen, J. Klafter and G. Zumofen, In Transport and Relaxation in Random Materials, Edited by J. Klafter, R. J. Rubin and M. F. Shlesinger. World Scientific, Philadelphia, PA. 1986. pp. 163-175.
11. D. B. Marshall, J. W. Burns, and D. E. Connolly. J. Am. Chem. Soc. 108, 1087 (1986).
12. C. H. Lochmüller, A. S. Colborn, M. L. Hunnicutt, and J. M. Harris, Anal. Chem. 55, 1344 (1983).
13. C. H. Lochmüller, A. S. Colborn, M. L. Hunnicutt and J. M. Harris, J. Am. Chem. Soc. 106, 4077 (1984).
14. M. L. Hunnicutt, J. M. Harris, and C. H. Lochmüller. J. Phys. Chem. 89, 5246 (1985).

15. A. L. Wong and J. M. Harris. Anal. Chem. 61, 2310 (1989).

16. W. H. Press, B. P. Flannery, S. A. Teukolsky, and W. T. Vetterling. Numerical Recipes. Cambridge University Press, New York, NY. 1987.

17. P. R. Bevington. Data Reduction and Error Analysis for the Physical Sciences. McGraw Hill, New York, NY. 1961.

18. S. W. Provencher. Comput. Phys. Commun. 27, 229 (1982).

19. D. W. Schaefer, J. E. Martin, P. Wiltzius, and D. S. Cannell. Phys. Rev. Lett. 52, 2371 (1984).

20. T. Freltoft, J. K. Kjems, and S. K. Sinha. Phys. Rev. 33B, 269 (1986).

21. D. R. James, Y. S. Liu, P. DE Mayo, and W. R. Ware, Chem. Phys. 120, 460 (1985).

22. L. R. Synder, Principles of Adsorption Chromotography. Marcel Dekker, Inc., New York. 1968.

23. A. L. Wong, J. M. Harris, J. Phys. Chem., submitted.

24. M. L. Hunnicutt, J. M. Harris, C. H. Lochmuller, J. Phys. Chem. 89, 5246 (1985).

25. F. W. Langkilde, E. W. Thulstrup, and J. Michl. J. Chem. Phys. 78, 3372 (1983).

26. R. D. Astumium, Z. A. Schelly, J. Am. Chem. Soc., 106, 304 (1984).

27. R. D. Astumium, Z. A. Schelly, J. Phys. Chem., 90, 537 (1986).

28. R. D. Astumian, P. B. Chuck, J. Phys. Chem. 89, 3477 (1985).

29. F. Castano, A. Lazaro, S. Lombrana, and E. Martinez, Spectra. Chem. Acta A. 395(1), 33 (1983).

30. K. C. Hartner, J. W. Carr, and J. M. Harris, Appl. Spectrosc., 43, 81 (1989).

Figure Captions

1. Fit of the last 85% of pyrene fluorescence decay data to a single exponential and a stretched exponential function with β fixed at 0.67. Silica suspension in methanol/iodine solution, $[I_2] = 5.41 \times 10^{-4}$ M. (a) fit of the fluorescence decay signal (points) to a single exponential (dashed line) and stretched exponential (solid line) functions, (b) weighted residuals of single exponential fit, (c) weighted residuals of stretched exponential fit.
2. Fit of the last 85% of immobilized pyrene fluorescence decay data to a stretched exponential function with β fixed at 0.67. (a) data (points) and stretched exponential model (solid line) and (b) weighted residuals.
3. Rate constant distribution for the unquenched and quenched pyrene fluorescence decay (i) $[I_2] = 0.0$, (j) $[I_2] = 0.197$ mM, (k) $[I_2] = 0.394$ mM, (m) $[I_2] = 0.591$ mM, and (n) $[I_2] = 0.788$ mM.
4. Stern-Volmer plot of the fluorescence decay rate of bound pyrene versus the concentration of iodine in methanol. Values of the decay rate were determined from nonlinear fit to a stretched exponential with $\beta = 0.67$ where $k = 1/\tau$ (squares), and from the mean of the rate distributions, $\langle k \rangle$ (triangles). The linear least-squares fits are shown (solid lines), where the quenching rate constant (k_q) is obtained from the slope.
5. Full width at half maximum of the rate distribution versus the most probable rate or mode of the distribution. X's are from Laplace inversion of the experimental decay curves. Squares are a homogeneous quenching model (Equation 6); and diamonds are from an inhomogeneous quenching model where k_o and k_q are correlated (Equation 7). Linear least squares fits to each set of results are shown; the one deviant experi-

mental point is not included in the fit since the number of counts in this experiment is small, resulting in a greater uncertainty in rate and a broader rate distribution.

6. Theoretical rate distributions based upon: (a) homogeneous quenching of the initially inhomogeneous population of surface fluors (Equation 6), and (b) an inhomogeneous quenching model where k_o and k_q are correlated (Equation 7).

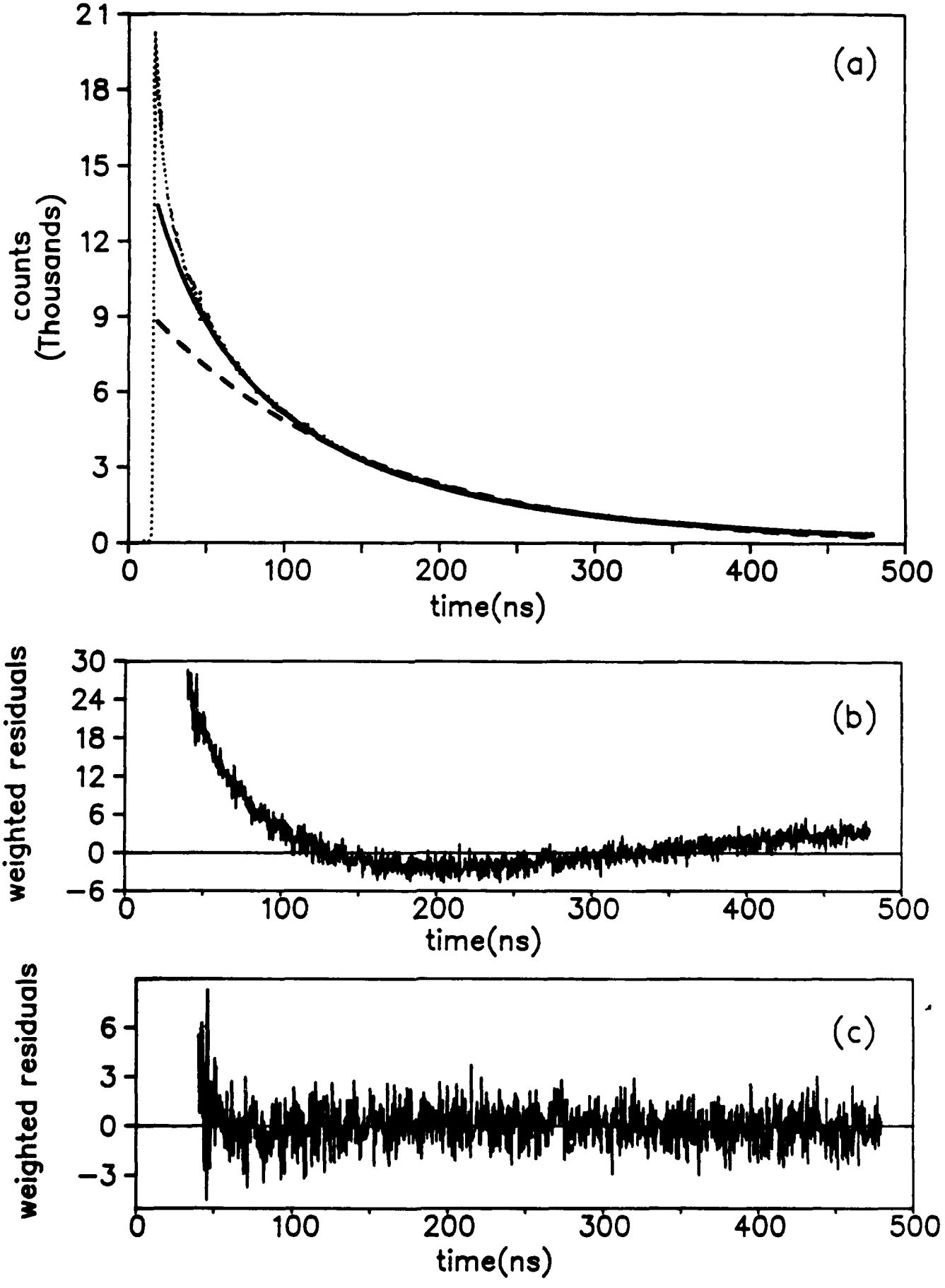
(a)
counts (Thousands)
21
18
15
12
9
6
3
0
0
100
200
300
400
500
time(ns)
(b)
weighted residuals
30
24
18
12
6
0
−6
0
100
200
300
400
500
time(ns)
(c)
weighted residuals
6
3
0
−3
0
100
200
300
400
500
time(ns)

Figure 1

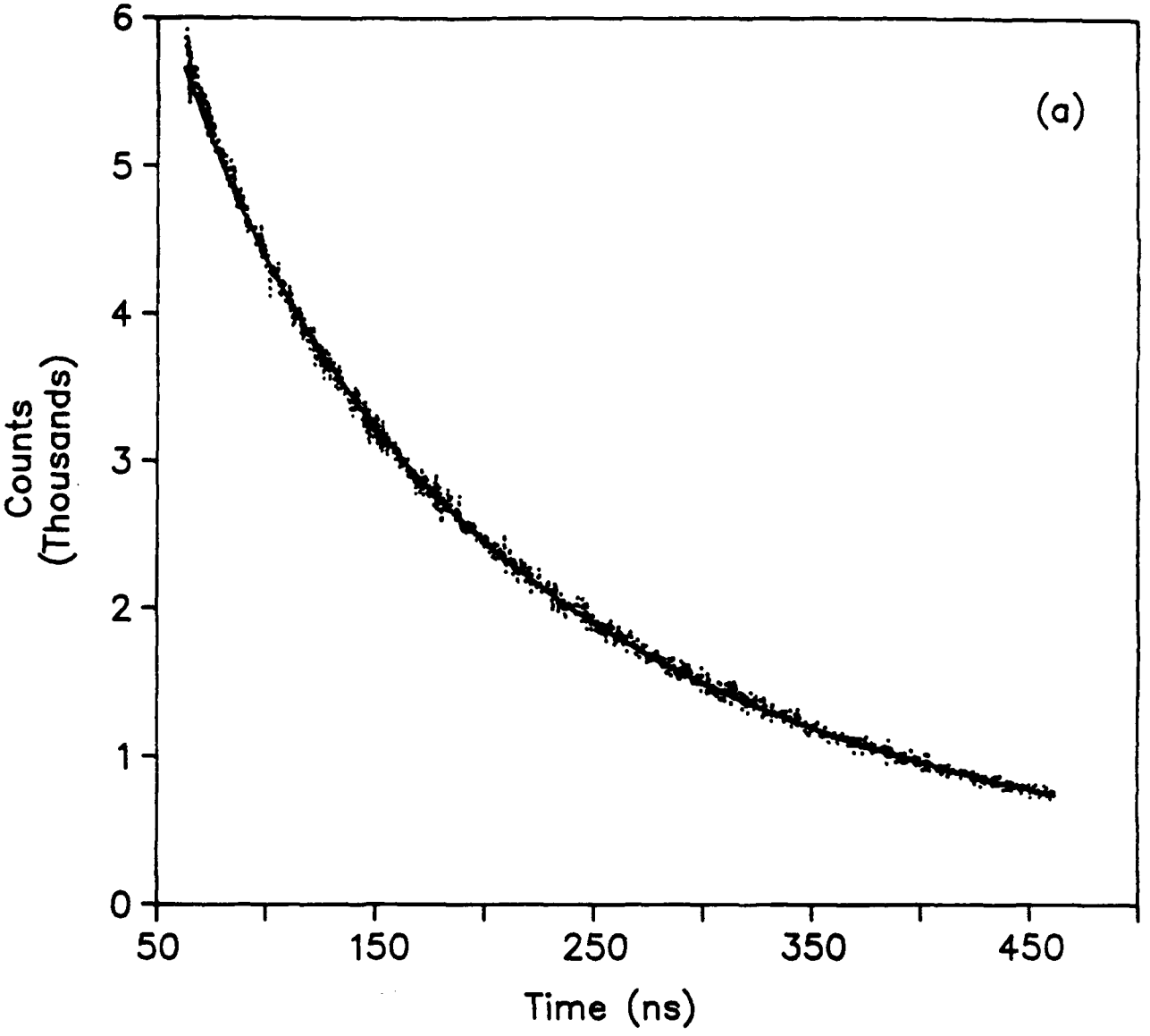
(a)
Counts (Thousands)
6
5
4
3
2
1
0
50
150
250
350
450
Time (ns)

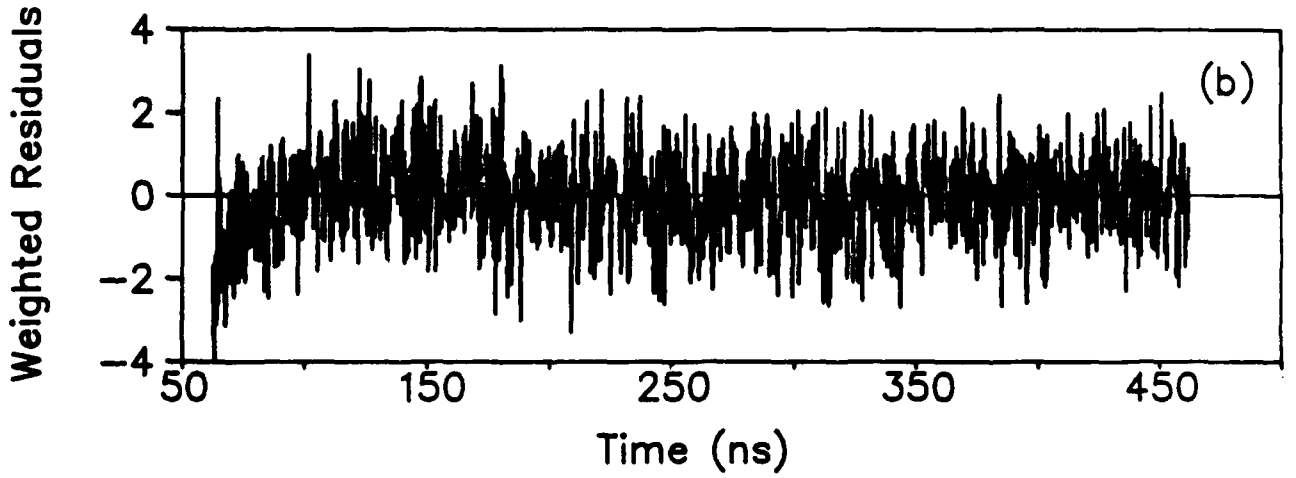
(b)
Weighted Residuals
4
2
0
−2
−4
50
150
250
350
450
Time (ns)

Figure 2

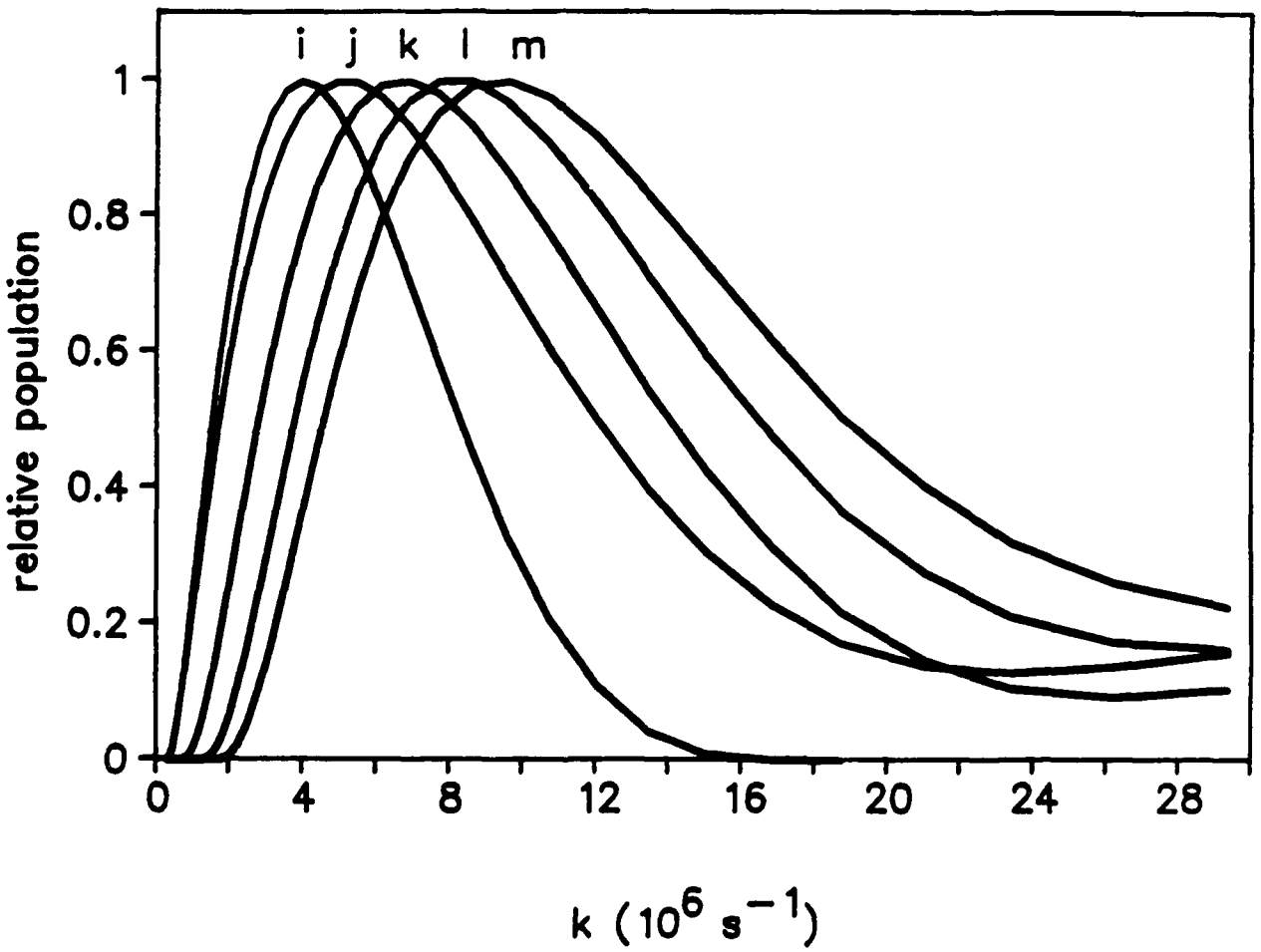
i j k l m
1
0.8
0.6
0.4
0.2
0
relative population
0
4
8
12
16
20
24
28
k (10^6 s^{-1})

Figure 3

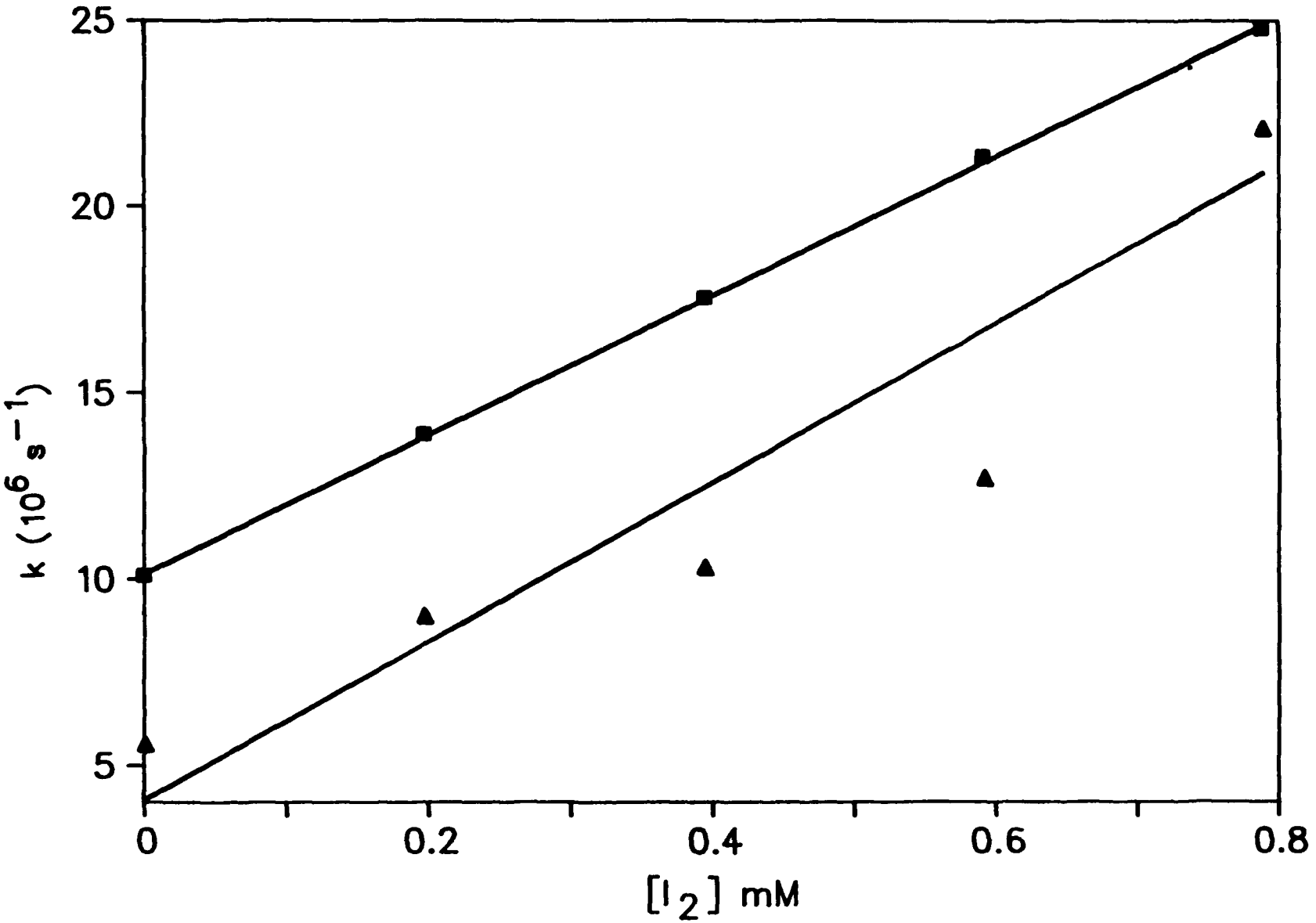
25
20
15
10
5
k (10^6 s^{-1})
0
0.2
0.4
0.6
0.8
[I_2] mM

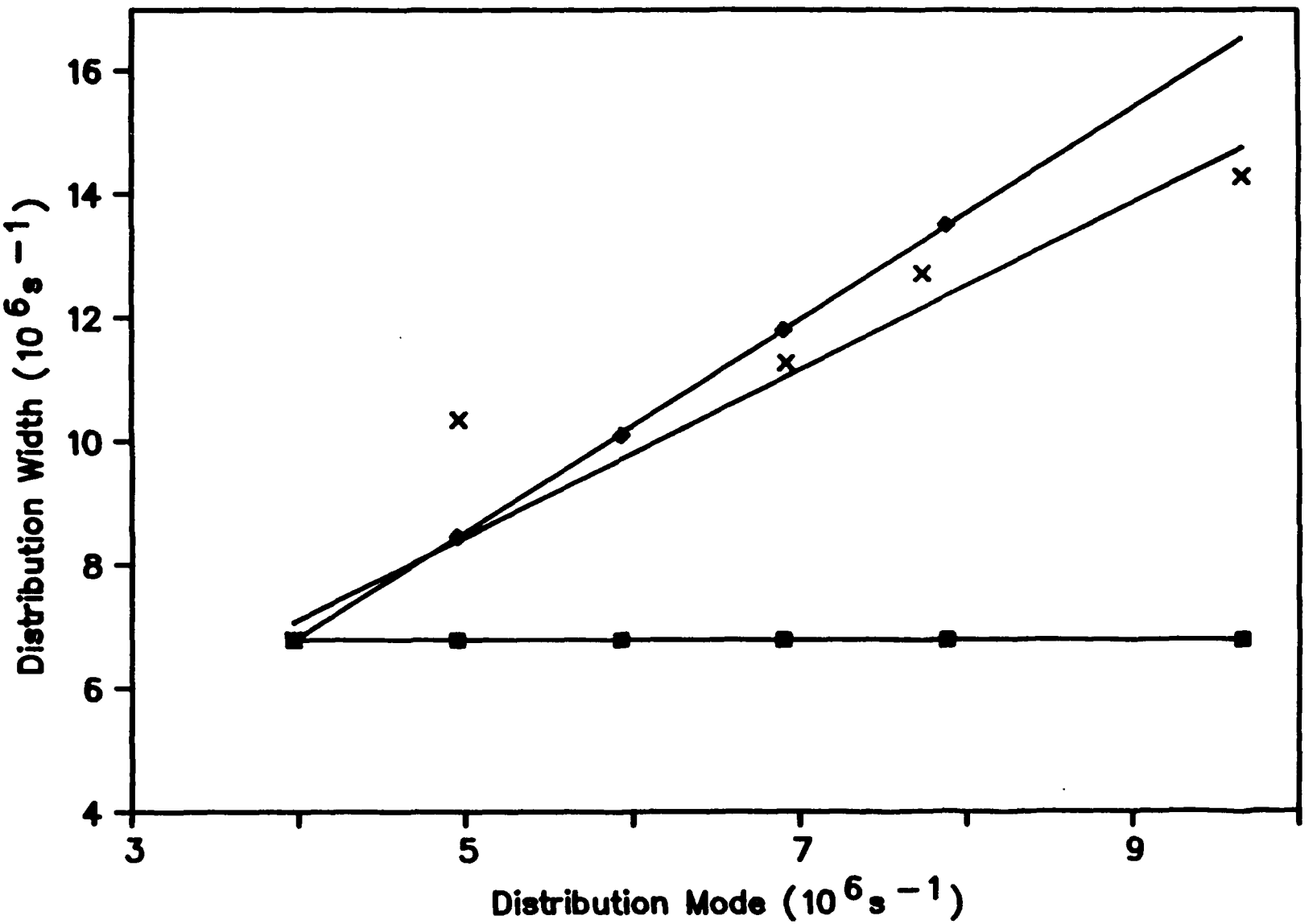
16
14
12
10
8
6
4
3
5
7
9
Distribution Width ($10^6 s^{-1}$)
Distribution Mode ($10^6 s^{-1}$)

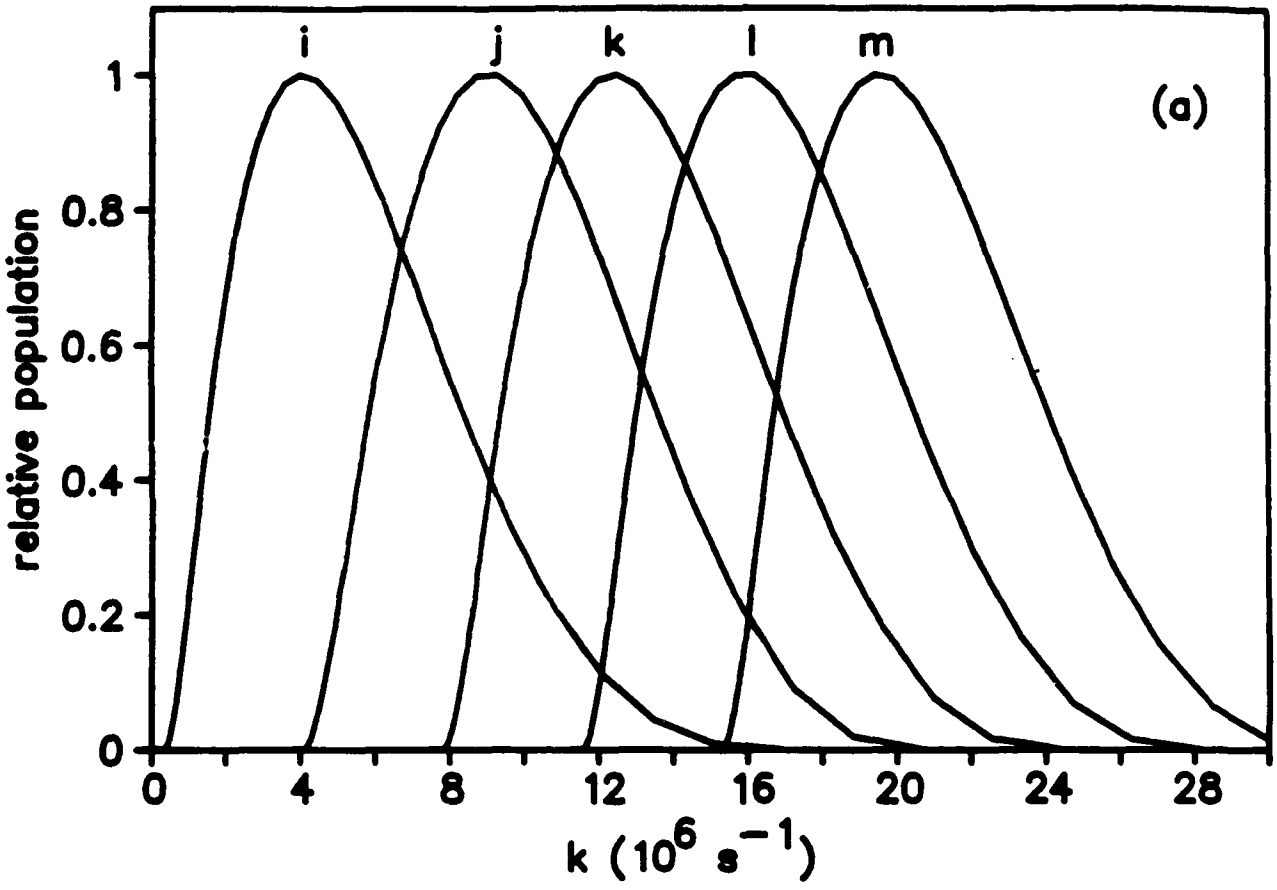
i
j
k
l
m
(a)
relative population
1
0.8
0.6
0.4
0.2
0
0
4
8
12
16
20
24
28
k (10^6 s^{-1})

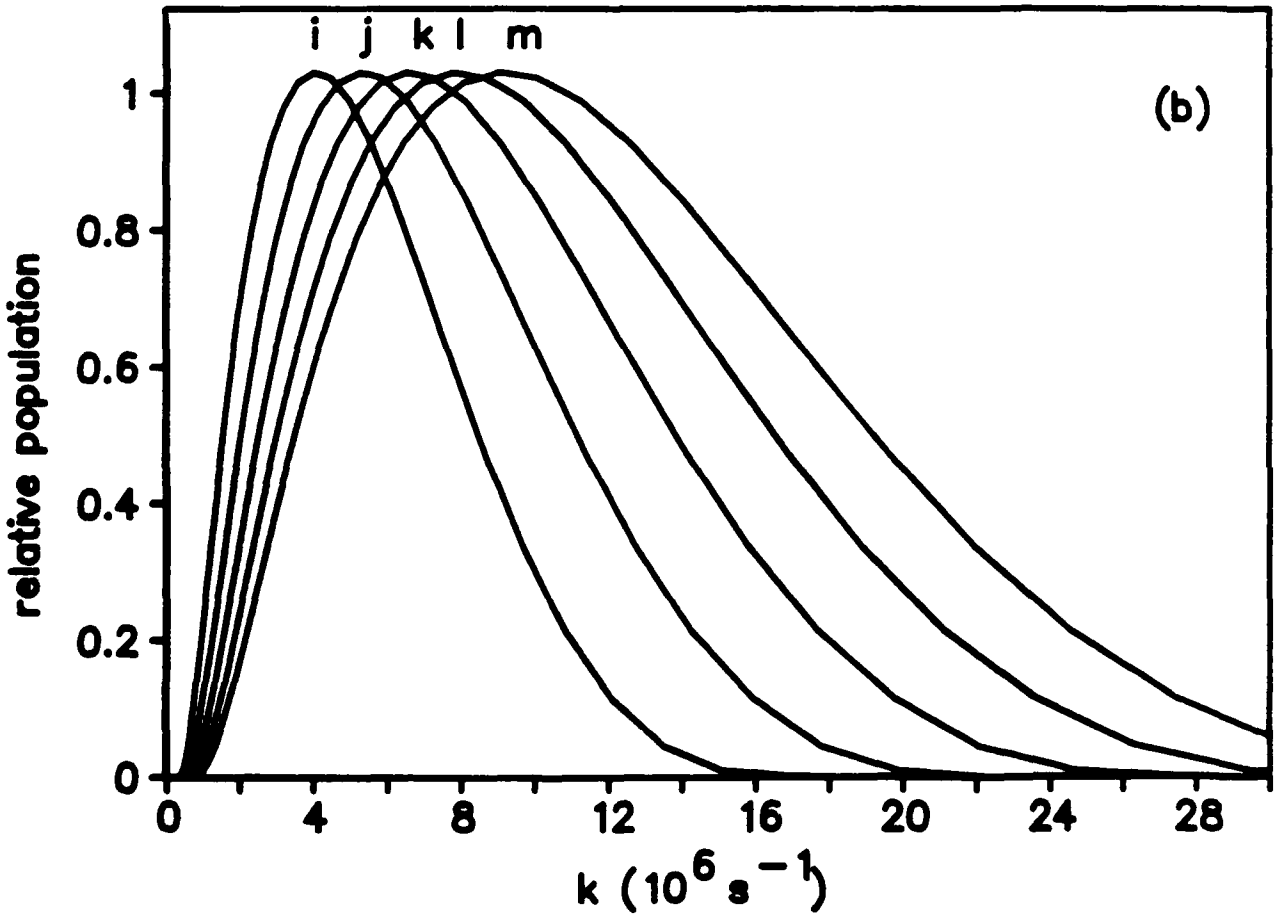
i j k l m
(b)
relative population
1
0.8
0.6
0.4
0.2
0
0
4
8
12
16
20
24
28
k (10^6 s^{-1})

Figure 6